Biol. Cybern. 79, 393–401 (1998)

Biological Cybernetics

A distributed control model for the air-righting reflex of a cat

Ara Arabyan, Derliang Tsai

Department of Aerospace and Mechanical Engineering, University of Arizona, Tucson, AZ 85721, USA

Received: 26 June 1995 / Accepted in revised form: 30 June 1998

Abstract. A multisegment, multijoint model of a falling animal is presented to examine the effectiveness of a two-stage control scheme in a zero-momentum self-righting maneuver. The model contains a much larger number of degrees of freedom than is required to execute a self-righting maneuver and is thus capable of providing multiple solutions for the same task. The decentralized control scheme is designed to achieve gross turning in minimum time and to maintain a steady orientation relative to gravity after the turn has been achieved. The scheme is able to determine the sequence of steps necessary to execute the motor task and also incorporates learning features. Results from various simulations are presented and their implications discussed.

1 Introduction

Animals and divers can change the spatial orientation of their bodies in the air without the benefit of net external torques by moving segments of their bodies in an appropriate manner. The sequence of individual body segment motions required to produce a specified turn without the use of external power sources is neither unique nor obvious and requires optimization and learning. The ability of an animal to right itself from an inverted position in free fall without the benefit of net external torques is known as the air-righting or self-righting reflex. In cases when the animal begins its free fall with no initial angular momentum, the self-righting maneuver is also known as a zero-angular-momentum turn, because no additional angular momentum is imparted to the animal during its fall. The air-righting reflex and the ability of different animals (including humans) to execute zero-angular-momentum turns has been studied by various researches in both the life and physical sciences. The phenomenon is interesting not just because it is not obvious, a priori, how such maneuvers can be executed using only relative motion between different segments of a multibody, multijoint system, but also because it poses a challenging control and optimization problem which may have applications in other areas (e.g., the reorientation of multisegment space vehicles).

The self-righting reflex of mammals in free fall was initially described by Marey (1894). Subsequently, the phenomenon was studied and recorded experimentally by Muller and Weed (1916) and Magnus (1922).

While past research on the subject proved the feasibility of zero-angular-momentum turns using simple two-cylinder models (e.g., Edwards 1986), the question of a general strategy and a control approach to the problem of reorienting a complex multisegment, multijoint system without the use of net external torques has remained largely unanswered. The difficulty in answering this question lies in the fact that, in general, there is an infinite number of ways a multisegment, multijoint system can be arbitrarily reoriented in space without the use of net external torques. Experimental kinematic data indicate that out of the many possible strategies to right themselves, animals use ones which have certain 'salient features' (Kane and Scher 1969). Any attempt to explain the control strategies used by animals in righting themselves has to take these salient features into account, and any motion resulting from any proposed control scheme must exhibit similar salient features. The salient features of the air-righting reflex which have been observed by various researchers and which are relevant to this study are:

1. The rotation in the air is initiated and executed by twisting and bending essentially two segments of the torso alternately or simultaneously.
2. The rotation takes place within as little space as the animal's standing height (McDonald 1960). When dropped from greater heights, the rotation still takes place within the first part of the motion (see sequence of photographs in Kane and Scher 1969).
3. Once the rotation takes place, the animal maintains a feet-down position throughout the rest of the fall regardless of the height it is dropped from.

Correspondence to: A. Arabyan
This research was partially supported by the National Science Foundation, grant no. ECS-9057062.

4. Visual and/or vestibular feedback mechanisms appear to be at work. Experiments show that cats which are blindfolded or have their inner ear mechanism disrupted can still execute the air-righting reflex, but not if both sensory apparatuses are disrupted (McDonald 1960).
5. Learning the maneuver through repeated trials improves the reliability of execution (O'Leary and Ravasio 1984).

In view of these observations, the following constraints were set on the control system that this study uses as a paradigm for the strategy used by animals in their air-righting maneuvers:

1. The turning part of the air-righting maneuver must be executed in minimum time (because of observation 2).
2. The turn must be stable, i.e., once the righting maneuver is complete, the model must be able to maintain a 'feet-down' position for the rest of the fall (because of observation 3). This is necessary because even though the total angular momentum of the system is zero at all times, the angular velocities and momenta of individual components in the system are not zero at all times, meaning that without this requirement, the momenta of the individual components could steer the overall system in an undesirable direction.
3. A decentralized scheme must be implemented to facilitate parallel control and computation (in order to have fast control and communication).
4. Some form position or velocity feedback is necessary initially to determine the initial orientation relative to a reference frame or gravity (because of observation 4).
5. The scheme must have provisions for learning the maneuver after repeated trials (because of observation 5).

2 Dynamic model

Figure 1 shows the principal components of the multisegment, multijoint cat model used in this study. The model consists of nine rigid bodies (B_i) and eight kinematic joints (J_i) of different types which determine the motions various segments of the animal's body relative to each other. It is evident that fewer or more bodies and joints could have been chosen to model the cat for the simulation of the air-righting reflex (indeed, two bodies with three joints are sufficient, as shown by Edwards 1986). This particular configuration was chosen in order to have components that roughly correspond to the different parts of the animal (head, feet, torso, etc.) and also to have a system which is complex enough to test the competence of the control system proposed.

The fore and hind limbs of the animal are modeled as single rigid bodies (B_6 and B_7) hinged by revolute joints (J_6 and J_7) to the front and rear segments of the torso (B_1 and B_5) which are linked to each other by a universal joint (J_4). A universal joint is one that permits relative

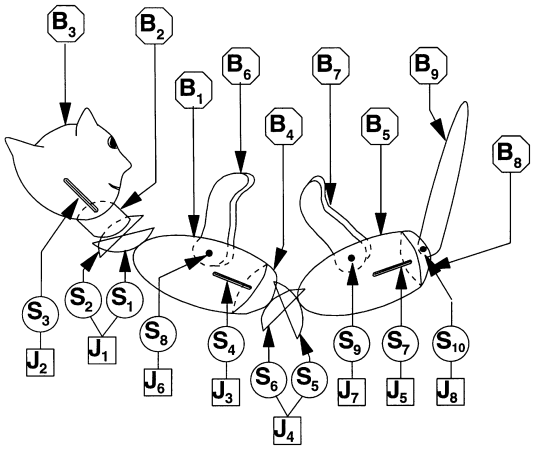

Fig. 1. Multisegment, multijoint model of a cat

rotations in two directions between the two bodies it connects. A schematic of a universal joint is shown in Fig. 2. The purpose of this joint is to allow the forward/backward and sideways flexion of the two torso segments relative to each other while transmitting a torque. A revolute joint (J_3) allows the twisting of the fore segment of the torso relative to the axes of J_4. The animal's head (B_3) is connected to a segment representing its neck (B_2) through a revolute joint (J_2), and the neck is connected to the front segment of the torso by another universal joint (J_1). Additionally, a tail assembly is attached to the posterior end of the rear segment of the torso by means of two noncolinear revolute joints (J_5 and J_8). All joints allow relative rotation between the two bodies they link in one direction only (1 degree of freedom), except J_1 and J_4 which permit relative rotations in two directions (2 degrees of freedom). The front segment of the torso is considered to be the base body whose orientation relative to the inertial frame determines the orientation of the cat. The masses and moments of inertia of each of the bodies in the model were based on anatomical data reported by Hoy and Zernicke (1985).

To account for the anatomical limits of motion at each joint and the presence of muscle, ligaments, and other tissue at and near the joints, nonlinear springs and dampers were included in the joints. Thus, each joint offers a resistance as a function of the relative position and velocity of the two bodies it links in the corresponding degree of freedom. The values for the joint stiffness and damping constants were chosen in accordance with the methods proposed by Lacquaniti and Soechting (1986).

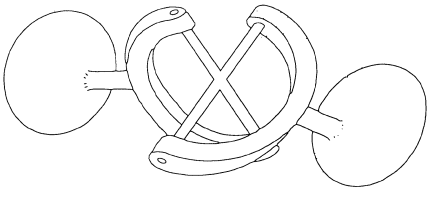

Fig. 2. A general universal joint

The entire system is driven by a set of actuators (S_i) which are placed at each of the joints and which control a single degree of freedom. Given that all degrees of freedom present in the system are rotational, all the actuators, or control susbsystems, are motors which can convert control signals into appropriate torques. It is assumed that the torque actuator i can apply is bounded by a maximum value, $U_{i\max}$.

In total, the system incorporates 16 rigid-body degrees of freedom and 10 control subsystems. The dynamics of the model is, in general, described by a set of coupled nonlinear differential and algebraic equations appropriate for modeling the dynamics of constrained multibody systems. These equations are of the form (Nikravesh 1989):

$$\begin{bmatrix} \boldsymbol{M} & \boldsymbol{\Phi}_{\mathbf{q}}^T \\ \boldsymbol{\Phi}_{\mathbf{q}} & 0 \end{bmatrix} \begin{bmatrix} \ddot{\mathbf{q}} \\ -\boldsymbol{\lambda} \end{bmatrix} = \begin{bmatrix} \mathbf{g} \\ -\boldsymbol{\gamma} \end{bmatrix} \tag{1}$$

where

$\mathbf{M}$ is the generalized inertia matrix of the system;
$\mathbf{q}$ is the generalized coordinate vector describing the configuration of the system in inertial space and $\ddot{\mathbf{q}}$ is the second time derivative of $\mathbf{q}$;
$\boldsymbol{\Phi}_{\mathbf{q}}$ is the Jacobian matrix that describes the constraints on the elements of $\mathbf{q}$;
$\boldsymbol{\lambda}$ is the vector of Lagrange multipliers;
$\mathbf{g}$ is the vector of external and internal generalized forces plus the nonlinear gyroscopic terms arising from coupling between the elements of $\mathbf{q}$; and
$\boldsymbol{\gamma}$ is the vector that results from differentiating the kinematic constraint equations twice with respect to time.

For a more detailed explanation of Equation 1, see the appendix.

3 Control scheme

Any control approach to achieve an overall turn of a multisegment, multijoint system using only internal forces or torques is complicated by the fact that any internal forces or torques applied at a joint will affect not just one segment but several others because of the dynamic coupling between them.

To comply with observations 1 and 2 above, a two-stage control scheme was implemented. The first stage is designed to change the orientation of the base body (B_1) from some starting position to a desired position in three-dimensional space, while the purpose of the second stage is to maintain the attitude of the base body and the limbs in the 'feet-down' position for the rest of the fall. The changeover from one stage to the other is determined by a coordinator on the basis of the value of a performance index, P, which is defined below. A block diagram of the overall scheme is shown in Fig. 3.

The first stage of control utilizes the actuators $S_3, S_4, S_5, S_7, S_8, S_9$, and S_{10} (see Fig. 4). Of these, S_3, S_4, and S_7, designated as *independent subsystems*, receive control commands from control modules U_3, U_4, and U_7 to produce appropriate torques which affect the associated bodies. For example, the torque produced by S_4 affects the motion of bodies B_1 and B_4. The control commands are governed by feedback from the position errors from *reference bodies* B_1, B_2 and B_5, each of which is one of the bodies affected by actuator subsystems S_3, S_4, and S_7. The independent subsystems are the actuators which control the inertially most dominant bodies in the system (i.e., the bodies which produce the greatest change in some specified performance index for a given change in angular orientation). The weighting functions W_1, W_2, and W_5 modify the measured errors in the orientation of bodies B_1, B_2, and B_5 in accordance with the inertial importance of these bodies in the particular maneuver. These may be considered as the 'software' which accounts for the relative weights and moments of inertia of the bodies and which can be reprogrammed for learning purposes.

The control laws for this stage are given by:

$$u_i = \begin{cases} -U_{i\max}\ \operatorname{sgn}(\theta_j - \theta_j^*) & \text{if } E_j = E_{\max} \\ \qquad i \in \{3,4,7\}; \quad j \in \{1,2,5\} & \\ -c_{1i}(\theta_j - \theta_j^*) - c_{2i}(\dot{\theta}_j - \dot{\theta}_j^*) & \text{if } E_j \neq E_{\max} \end{cases} \tag{2}$$

$$E_j = |W_j(\theta_j - \theta_j^*)| \tag{3}$$

$$E_{\max} = \max(E_1, E_2, E_5) \tag{4}$$

$$P = E_1 + E_2 + E_5 \tag{5}$$

where

u_i is the torque produced by actuator S_i;
$U_{i\max}$ is the maximum torque actuator S_i may apply;
θ_j is the actual orientation (relative to a fixed inertial frame) of the reference body associated with S_i;
θ_j^* is the desired orientation of the reference body associated with S_i;
$\dot{\theta}_j$ is the actual rate of rotation of the reference body associated with S_i;
$\dot{\theta}_j^*$ is the desired rate of rotation of the reference body associated with S_i;
W_j is the weighting function associated with the inertial importance of body B_j;
P is the performance index; and
c_{1i} and c_{2i} are constants proportional to the stiffness and damping associated with the degree of freedom controlled by actuator S_i.

Actuator subsystems S_5, S_8, S_9, and S_{10}, designated as *dependent subsystems*, apply concurrent torques on their associated bodies in accordance with an algorithm which attempts to minimize or maximize a local function. For example, for this particular air-righting maneuver, subsystem S_9 acts in a way that minimizes the combined moment of inertia of bodies B_5 and B_7 (hind legs) about the current axis of rotation in minimum time. The control commands sent by the dependent control modules are functions of modifying factors F_i (see Fig. 4) which are, in general, programmable, and their programs depend on which independent actuator is

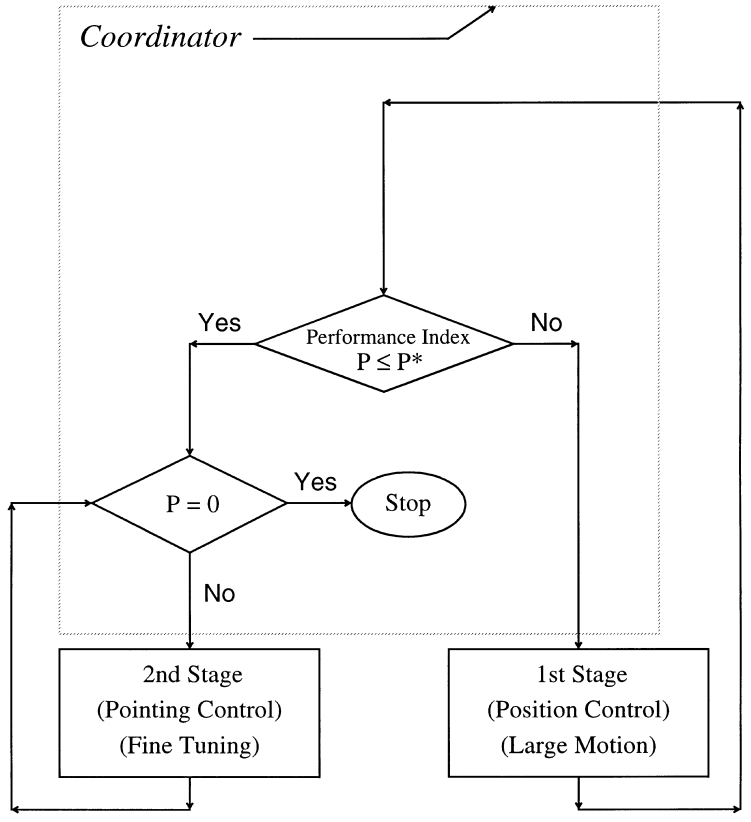

Fig. 3. Two-stage control scheme

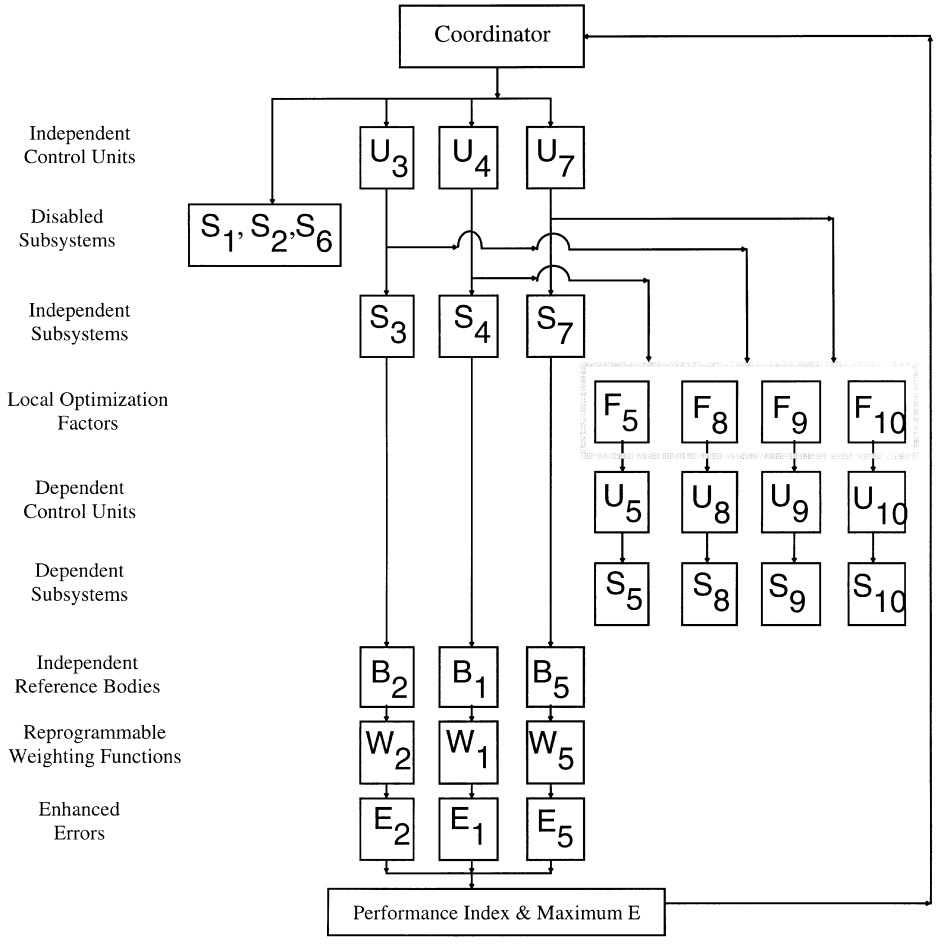

Fig. 4. Decentralized large motion control

acting at a given time. The modifying factors F_i can also be reprogrammed through a local feedback loop and may be considered as local optimization modules.

Some actuator subsystems (S_1, S_2, S_6) are disabled. This is done to reduce computation and control feedback time, and they are so selected because the bodies with which they are associated are not inertially important for this particular maneuver. It is obvious that this disabling can be accomplished by setting the corresponding weighting functions W_i to zero to reflect the low inertial importance of their associated bodies. This would set the enhanced error E_i for their associated bodies to zero, and thus no error for those bodies would be fed back, requiring no correction by the actuator subsystems driving them.

The second stage of control is a linear feedback control system which maintains the attitude of the entire system stable around a desirable position (see Fig. 5). It is possible to use linear feedback in this stage because the deviations or errors from the desired position (which corresponds to a stable equilibrium configuration) are small. In this stage, only two actuator subsystem (S_1, S_7) are active; the rest of the actuator subsystems are disabled to reduce computation times. The error from the desired position is measured on the basis of the orientations of bodies B_1, B_2, and B_5. The control torques in this stage are given by:

$$u_i = -c_{1i}(\theta_j - \theta_j^*) - c_{2i}(\dot{\theta}_j - \dot{\theta}_j^*) \quad i \in \{1,7\}; \quad j \in \{1,2,5\} \tag{6}$$

where c_{1i} and c_{2i} are constants proportional to the stiffness and damping present in actuator S_i.

In both stages of control, all actuator torques are bounded so that no actuator can exert a torque larger than its capacity. For minimum-time large motion control, this requires that any active actuators exert the maximum torque they can. This is equivalent to 'bang-bang control'. Only the actuator that is associated with the body with the largest error from the desired position is activated with the maximum torque available for that actuator. The other independent actuators exert torques proportional to the spring and damper in them, as proposed Lacquaniti and Soechting (1986).

4 Learning and optimization

As shown in Fig. 4, the positional errors from the various bodies in the system are modified by weighting factors W_i to account for their inertial importance in a given maneuver. It is obvious that the weighting factors have to be different in each different type of maneuver and even in different stages of the same maneuver. Because of the way they are used in computing the

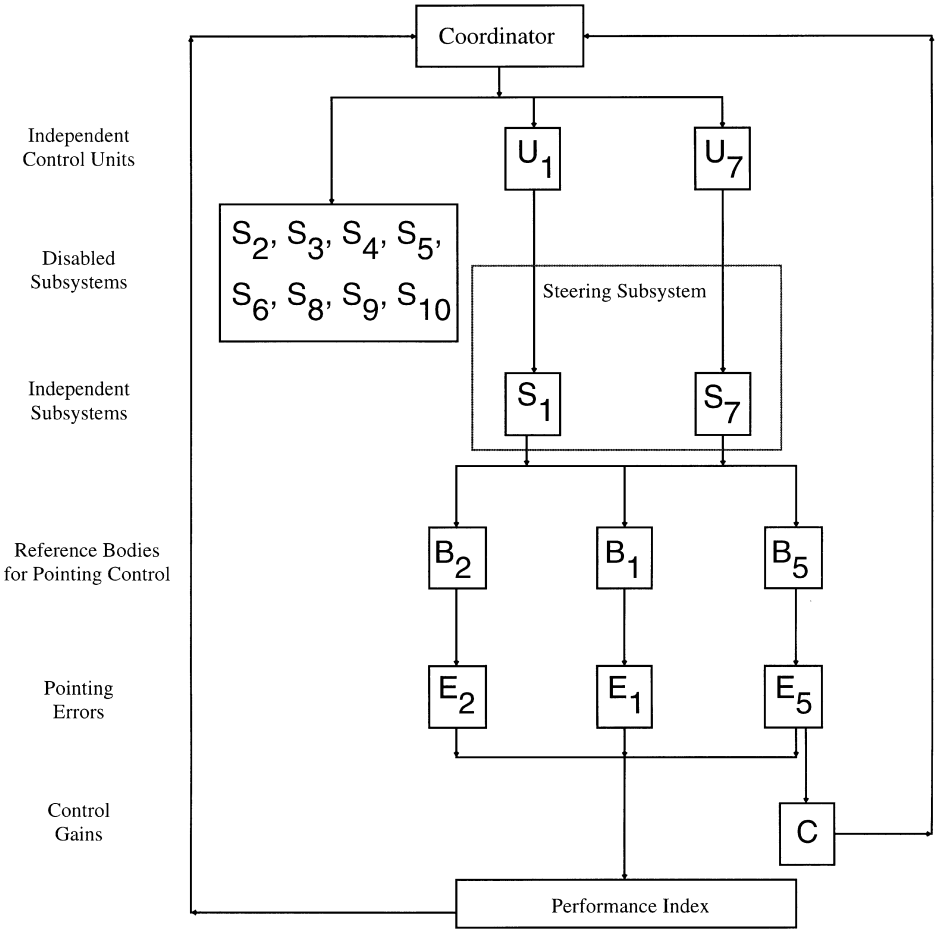

Fig. 5. Closed-loop fine tuning control

performance index, these weighting factors serve as the system's 'knowledge' about which bodies to use as references and which as dependent subsystems (the errors from those bodies have weighting factors of zero). This raises the question of how these factors should be decided.

In the present model, these factors were chosen to be proportional to the masses and moments of inertia of each of the bodies, and only the bodies with the largest masses and moments of inertia were assigned nonzero weighting factors. Conversely, these factors may serve as programming devices to make the system learn about itself, modifying them after each maneuver until they have values which make the maneuver 'optimal' in some sense defined by the system.

The weighting factors F_i also play a similar role and must be set differently in each different maneuver. However, since these factors affect only the dependent subsystems, their setting must be determined locally with an eye to maximizing or minimizing some local objective function. It is known that biological systems do, in fact, maintain such local control and optimization schemes, and it has been suggested that this is necessary for rapid response and stability (e.g., Hogan 1990). In this model, these weighting factors were once again set to the moments of inertia of bodies B_6 and B_7 around the axes of joints J_6 and J_7, respectively, and the objective function to be minimized was chosen as the total moment of inertia around the global axis of rotation. This simple objective function was chosen to minimize the time of rotation which was deduced heuristically from observation 2 above.

5 Results

The results of a simulation of the model in the control scheme described above are shown in Figs. 6–10. Figure 6 is a sequence of selected frames from an animation of the model based on the orientations of the different segments computed using the scheme described above. Though not verifiable by experiment, the figure describes clearly the resulting motion which complies to a large extent with observations 1–3 enumerated in Sect. 1. Figure 7 shows the time history of the torques in actuators that control the independent bodies in the system during the first stage of control. These actuators are active only until most of the desired large motion is accomplished (i.e., when the performance index, P, drops below a specified value). S_3 and S_4 exert constant torques for most of the large motion, while S_7 alternately applies the maximum torque it has available in positive and negative directions. Subsystem S_7 is predominantly active because the maximum enhanced error $E_{\max}$, which determines what independent subsystem must apply the maximum torque, is E_5 during most of the maneuver. This occurs because the weighting function W_5 is large (to account for the large mass of B_5 which is controlled

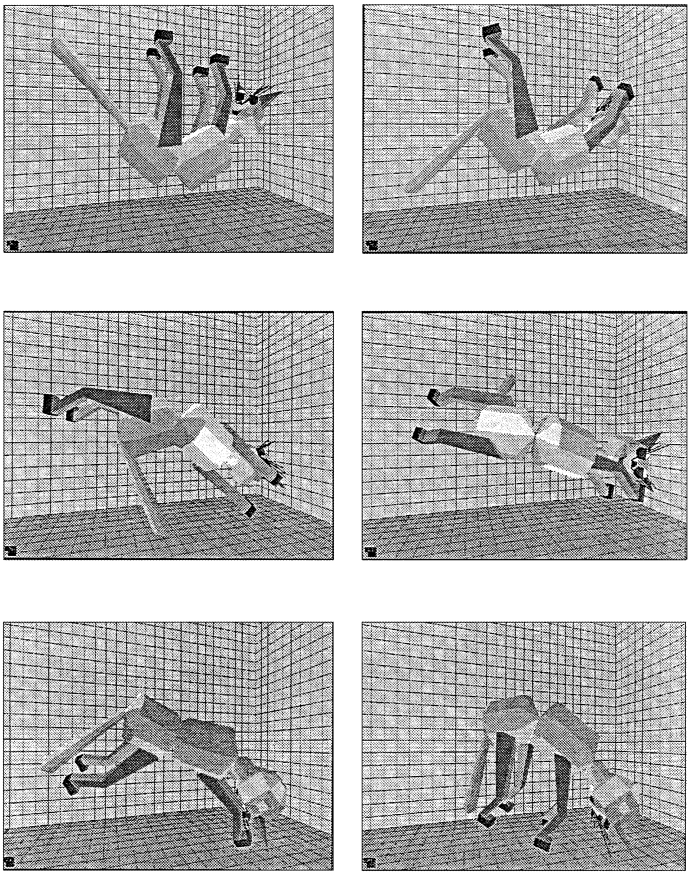

Fig. 6. A sequence of selected frames from a simulation run

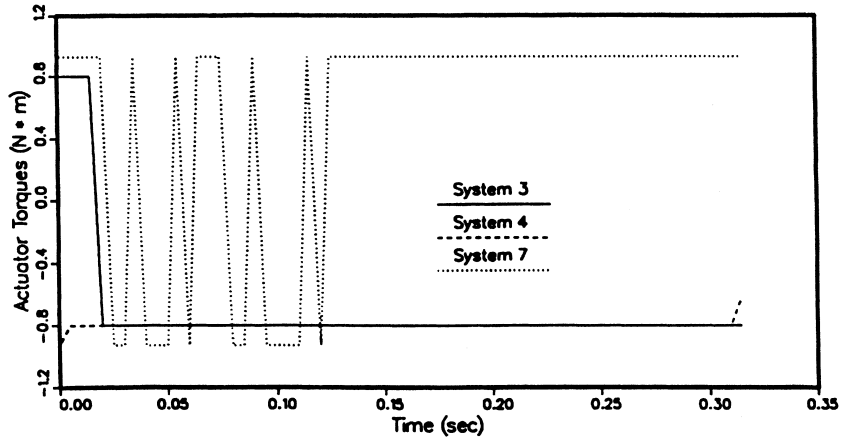

Fig. 7. Variation of independent actuator torques with time (large motion control)

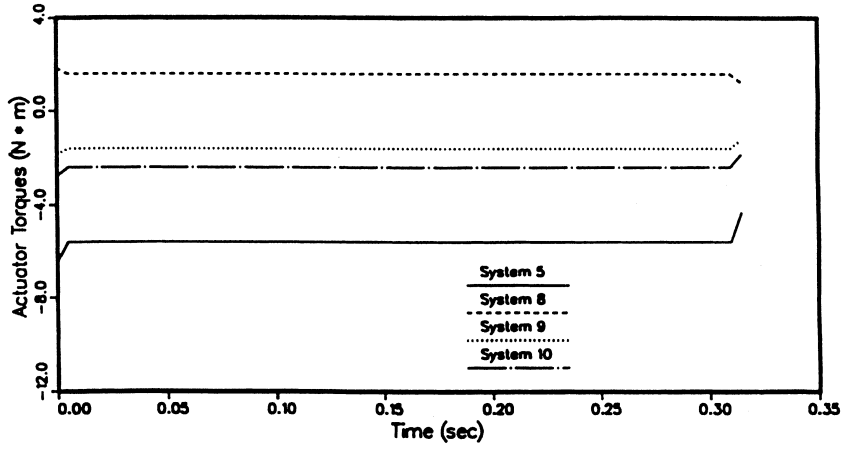

Fig. 8. Variation of dependent actuator torques with time (large motion control)

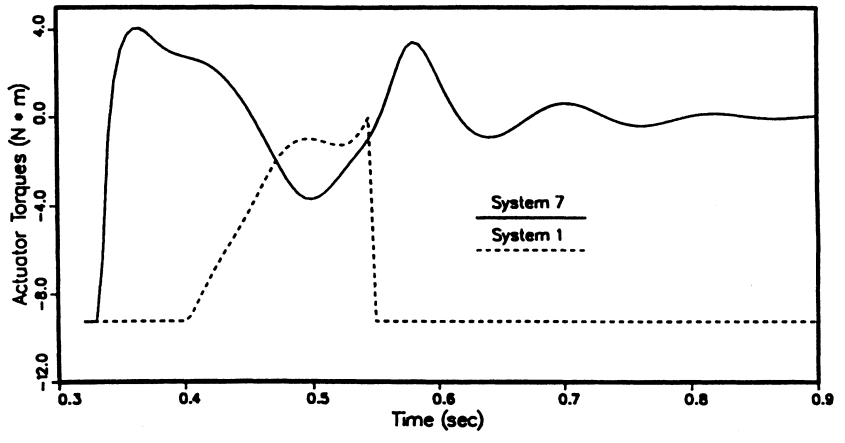

Fig. 9. Variation of active actuator torques with time (fine tuning control)

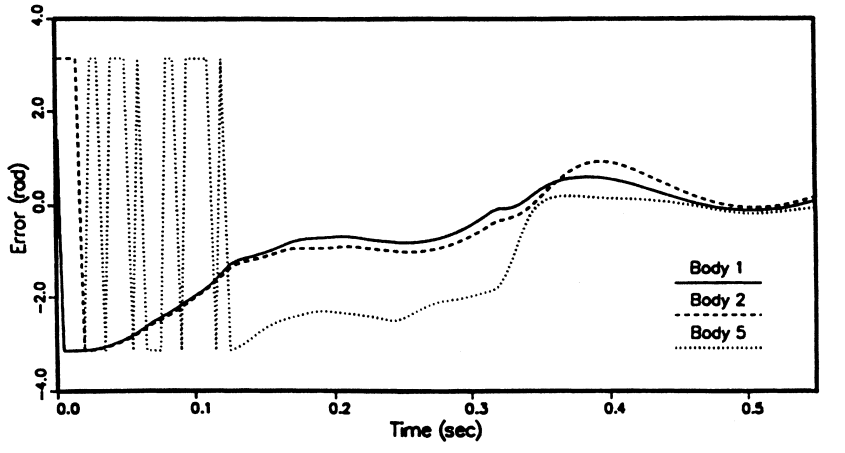

Fig. 10. Variation of reference body position errors target orientation

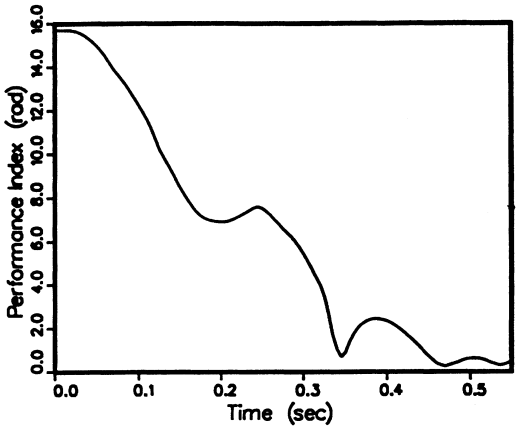

Fig. 11. Decline of the performance index over time

by S_7) compared with W_1 and W_2. The maximum torque applied by S_7 is initially applied alternately in the positive and negative directions because the desired reorientation objective can be achieved by turning B_5 in either direction, and the system does not 'know' which way to turn. Eventually, after a few tries, the performance index P is reduced sufficiently in one direction, and that direction is chosen. During the same interval, the dependent subsystems S_5, S_8, S_9, and S_{10} apply relatively flat torques (Fig. 8) to minimize the moment of inertia of the body systems they control about the desired axis of rotation.

The time history of torques exerted by the active subsystems during the second stage of control is shown in Fig. 9. These subsystems control bodies B_1, B_2, and B_5, and their torques are governed by the largest enhanced error computed for these bodies. Once again, the error from B_5 dominates the control.

Figure 10 shows the reduction in the position errors for the three reference bodies B_1, B_2, and B_5 relative to the target orientation. The figure indicates that initially B_5 rotates about the desired orientation by large variations, but in fact it is changing its orientation by a small amount from its initial orientation (π radians from the target orientation) in the positive and negative directions, which is mathematically equivalent to roughly $\pm\pi$ radians from the target orientation.

Lastly, Fig. 11 depicts the decline of the performance index, P (which is measure of the compositive 'error'), as the system moves from its original configuration toward the target configuration. The second stage of the control system kicks in at around 0.35 s when P has declined to below the preset error tolerance.

6 Conclusions

A multisegment, multijoint model of a falling animal together with a two-stage control system has been constructed. The system is capable of executing zero-momentum angular turns, simulating the animal's self-righting reflex autonomously using only simple feedback schemes. The executed turns exhibit the salient features of a cat's air-righting reflex as reported by other researchers: The large motion of the turn is executed with a strategy that tries to achieve the rotation in minimum time (i.e., by minimizing the total moment of inertia of the system about the global axis of rotation). However, minimum time is not achieved strictly because of the concurrent action of subsystems. The animal stays in the desired final orientation for the rest of the fall with minimal control. The system incorporates features whereby the model can reprogram itself in repeated trials to improve its performance. In addition, the use of autonomous subsystems offers the possibility of distributed computing and control.

Appendix

Consider a system composed of n rigid bodies that are free to move in three-dimensional space. Let $\mathbf{x}_i = [x_i, y_i, z_i]^T$ and $\boldsymbol{\theta}_i = [\theta_i, \phi_i, \psi_i]$ represent the position of the center of mass and the angular orientation of body i relative to an inertial frame, respectively. The elements of $\boldsymbol{\theta}_i$ may be any set of consistent angular measures such as Euler angles. Then, the translational motion of the body can be described by Newton's second law of motion:

$$m_i \ddot{\mathbf{x}}_i = \mathbf{f}_i(t) \tag{7}$$

where m_i is the mass of body $i, \ddot{\mathbf{x}}_i = \frac{d^2\mathbf{x}}{dt^2}$, and $\mathbf{f}_i$ is the 3×1 vector of the resultant external forces acting on the body.

Also, the rotational motion of the body can be described by Euler's equations:

$$\mathbf{I}_i \dot{\boldsymbol{\omega}}_i = \mathbf{n}_i(t) - \boldsymbol{\omega}_i \times \mathbf{I}_i \boldsymbol{\omega}_i \tag{8}$$

where $\boldsymbol{\omega}_i$ is the angular velocity vector of body i, measured in an inertial frame but referred to an orthogonal reference frame fixed in body $i, \dot{\boldsymbol{\omega}}_i = \frac{d\boldsymbol{\omega}_i}{dt}$, $\mathbf{I}_i$ is the 3×3 moment of inertial matrix of body i; and $\mathbf{n}_i$ is the vector of the resultant external moments acting on body i. It can be shown that, in general $\boldsymbol{\omega}_i = \mathbf{G}_i(\boldsymbol{\theta}_i)\dot{\boldsymbol{\theta}}_i$ where $\mathbf{G}_i$ is an invertible 3×3 matrix that transforms coordinates from the fixed inertial reference frame to the body-fixed reference frame.

Now, the equations of motion for body i can be written in compact form as:

$$\mathbf{M}_i \ddot{\mathbf{q}}_i = \mathbf{g}_i(\mathbf{q}_i, \dot{\mathbf{q}}_i, t) \tag{9}$$

where $\mathbf{q}_i = [\mathbf{x}_i{}^T \theta_i{}^T]^T$, and $\mathbf{g}_i$ includes $\mathbf{f}_i, \mathbf{n}_i$, and the gyroscopic terms [second term on right-hand side of (8)]. In (9), $\mathbf{M}_i$ is a 6×6 matrix given by:

$$\mathbf{M}_i = \begin{bmatrix} m_i & 0 & 0 & \dots \\ 0 & m_i & 0 & \dots \\ 0 & 0 & m_i & \dots \\ \dots & \dots & \dots & \mathbf{I}_i \end{bmatrix} \tag{10}$$

Now suppose that the motion of the n bodies considered above is constrained such that the elements of $\mathbf{q}_i$ $(i = 1, 2, \dots, n)$ are no longer independent. If there are m such constraints, they can be expressed most generally in the form of a set of nonlinear algebraic equations (holonomic constraints):

$$\phi_j(\mathbf{q}_1, \mathbf{q}_2, \dots, \mathbf{q}_n) = 0 \quad j = 1, 2, \dots, m \tag{11}$$

This can be written in more compact form as:

$$\boldsymbol{\phi}(\mathbf{q}) = 0 \tag{12}$$

where now $\boldsymbol{\phi}$ is an $m \times 1$ vector function of the $6n$ elements of the vector

$$\mathbf{q} = [\mathbf{q}_1{}^T, \mathbf{q}_2{}^T, \ldots, \mathbf{q}_n{}^T]^T.$$

The equations of motion for the n free bodies in (10) can be combined with the m constraints in (12) using the method of Lagrange multipliers to obtain:

$$\begin{bmatrix} \mathbf{M} & \boldsymbol{\Phi}_{\mathbf{q}}^T \\ \boldsymbol{\Phi}_{\mathbf{q}} & 0 \end{bmatrix} \begin{bmatrix} \ddot{\mathbf{q}} \\ -\boldsymbol{\lambda} \end{bmatrix} = \begin{bmatrix} \mathbf{g} \\ -\boldsymbol{\gamma} \end{bmatrix} \tag{13}$$

where now $\mathbf{M}$ is a $6n \times 6n$ global mass matrix made up of concatenating $\mathbf{M}_i$ diagonally; $\mathbf{g}$ is a $6n \times 1$ vector obtained by concatenating $\mathbf{g}_i$; $\boldsymbol{\lambda}$ is the $m \times 1$ vector of Lagrange multipliers; $\boldsymbol{\Phi}_{\mathbf{q}} = \frac{\partial \boldsymbol{\Phi}}{\partial \mathbf{q}}$ and $\boldsymbol{\gamma} = \boldsymbol{\Phi}_{\mathbf{q}} \dot{\mathbf{q}}$. The $m \times n$ matrix $\boldsymbol{\Phi}_{\mathbf{q}}$ is known as the Jacobian of $\boldsymbol{\phi}$ with respect to $\mathbf{q}$ (Nikravesh 1988; Shabana 1989).

Equation (13) represents a differential-algebraic system of equations in $6n + m$ unknowns, with the differential portion made up of $6n$ coupled, nonlinear, ordinary differential equations. Knowing the external forces and moments acting on individual bodies at any time and the initial conditions for the system, (13) can be solved for $\mathbf{q}(t), \dot{\mathbf{q}}(t)$ and $\boldsymbol{\lambda}(t)$ using appropriate numerical methods (see Petzold 1983; Shabana 1989). In this modeling example, if a control torque exerted by actuator S_i affects bodies B_j and B_k, it is included in (13) as an external torque for body j in $\mathbf{g}_j$ and an equal but opposite external torque on body k in $\mathbf{g}_k$. The equations are then numerically inverted and integrated for one time step, at which time all quantities are updated in accordance with the control laws and independent external forces. Also, in this case, Euler parameters rather than real angles were used to represent the orientation of each body in inertial space. The reason for this is that Euler parameters (a set of four parameters subject to one algebraic constraint) exhibit much better behavior in numerical analysis and are unlikely to cause any numerical instabilities as, for example, Euler angles [see Goldstein (1980) and Nikravesh (1988) for a discussion of Euler parameters and their use].

References

Edwards MH (1986) Zero angular momentum turns. Am J Phys 54:846–847

Goldstein H (1980) Classical mechanics, 2nd ed. Addition-Wesley, Reading, Mass

Hogan N (1990) Mechanical impedance of single and multi-articular systems. In: Winter JM, Woo SLY (eds) Multiple muscle systems. Springer Berlin Heidelberg, New York

Hoy MG, Zernicke RF (1985) Modulation of limb dynamics in the swing phase of locomotion, J Biomech 18:49–60

Kane TR, Scher MP (1969) A dynamical explanation of the falling cat phenomenon. Int J Solids Structures 5:663–670

Kane TR, Scher MP (1970) Human self-rotation by means of limb movements. J Biomech 3:39–49

Lacquaniti F, Soechting JF (1986) Simulation studies on the control of posture and movement in a multi-jointed limb. Biol Cybern 54:367–378

Magnus R (1922) Wie sich die fallende Katze in der Luft umdreht, Arch Neerl Physiol 7:218–222

Marey M (1894) Des mouvements que certains animaux pour retomber sur leurs pieds, lorsqu'ils son precipités d'un lieu élevé. Compt Rend Acad Sci Paris 119:714–717

McDonald D (1960) How does a cat fall on its feet? New Scientist, 7:1647–1649

Muller HR, Weed LH (1916) Notes on the falling reflex of cats. Am J Physiol 40:373–379

Nikravesh PE (1988) Computer-aided analysis of mechanical systems. Prentice Hall, Englewood Cliffs, NJ

O'Leary DP, Ravasio MJ (1984) Simulation of vestibular semicircular responses during righting movement of a freely falling cat. Biol Cybern 50:1–7

Petzold LR (1983) A description of DASSL: a differential/algebraic system solver. In: Stepleman RS, et al (eds) Scientific computing. North-Holland, Amsterdam, pp 65–68

Shabana AA (1989) Dynamics of multibody systems. John Wiley, New York, pp 390–433